

# A unified treatment of derivative discontinuity, delocalization and static correlation effects in density functional calculations

Fei Zhou(周 非)\*

*Physical and Life Sciences Directorate,*

*Lawrence Livermore National Laboratory, Livermore, CA 94550, USA*

Vidvuds Ozoliņš†

*Department of Applied Physics, Yale University, New Haven, CT 06520, USA and*

*Yale Energy Sciences Institute, Yale University, West Haven, CT 06516, USA*

(Dated: December 14, 2024)

## Abstract

We propose a method that incorporates explicit derivative discontinuity of the total energy with respect to the number of electrons and treats both delocalization and static correlation effects in density functional calculations. Our approach is motivated by the exact behavior of the ground state total energy of electrons and involves minimization of the exchange-correlation energy with respect to the Fock space density matrix. The resulting density matrix minimization (DMM) model is simple to implement and can be solved uniquely and efficiently. In a case study of  $\text{KCuF}_3$ , a prototypical Mott-insulator with strong correlation, LDA+DMM correctly reproduced the Mott-Hubbard gap, magnetic ordering and Jahn-Teller distortion.

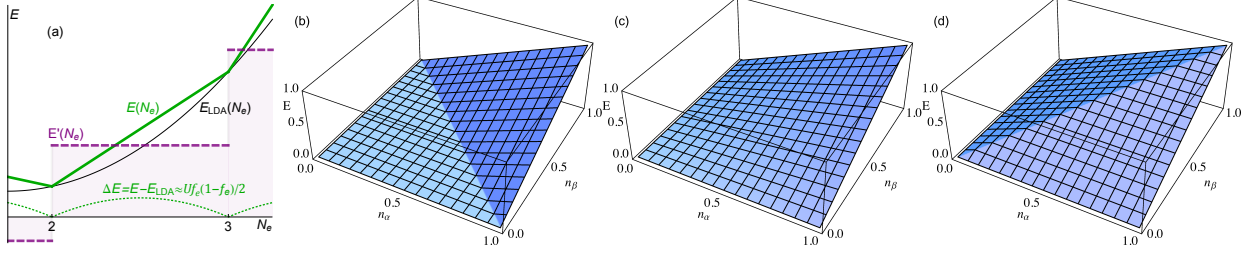


FIG. 1. (a) Schematic energy vs.  $N_e$ , and comparison of  $s$ -electron Coulomb energy  $E_{ee}$  with  $U = 1$  and  $\mathbf{n} = \text{diag}(n_\alpha, n_\beta)$  minimized by (b) Eq. 2, (c) mean-field  $n_\alpha n_\beta U$ , and (d) the idempotent constraint of Eq. 3.

Despite its enormous success in computational physics, chemistry and materials science, density functional theory (DFT) is still plagued by major setbacks in strongly correlated systems, where the many-body nature of the electronic interactions manifests itself and leads to well-documented qualitative failures of the local density and generalized gradient approximations (LDA, GGA) to the exchange-correlation (xc) functional [1–3]. Inspired by sustained progress in strong correlation physics, e.g. on the Hubbard model, so-called “beyond DFT” approaches have been developed, including LDA+ $U$  [4], LDA plus the dynamic mean-field theory (LDA+DMFT) [5, 6], and LDA plus the Gutzwiller approximation (LDA+GA) [7, 8], to name a few [9]. The widely adopted LDA+ $U$  method correctly opens up a band gap for certain Mott insulators, a significant achievement at the time of its introduction. The more advanced LDA+DMFT method, incorporating dynamic on-site correlations beyond LDA+ $U$ , has been very successful in reproducing the electronic spectral properties of strongly correlated systems and has significantly contributed to our current understanding of high- $T_c$  superconductors [5, 6]. Similarly, LDA+GA has achieved successes in strongly correlated systems [10].

In this work, we approach the correlation problem by revisiting the foundations of DFT, i.e., the behavior of the exact ground-state energy  $E$ . First,  $E$  should be piecewise linear in the number of electrons  $N_e$ , with discontinuity in  $dE/dN_e$  at integer  $N_e$  [11, 12]. This famous *derivative discontinuity* [11–14], or the fundamental band gap, is absent in LDA/GGA due to the self-interaction/delocalization error, leading to underestimated charge localization and band gaps at integer  $N_e$  (see Fig. 1a). In DFT, the band gap is given by the Kohn-Sham

(KS) eigenvalue gap plus an *explicit* discontinuity from the xc functional [13, 14]:

$$E_g = \epsilon_{N_e+1}^{\text{KS}} - \epsilon_{N_e}^{\text{KS}} + \mathcal{D}_{\text{xc}}. \quad (1)$$

This means that even if the exact KS gap were known, there is still a missing discontinuity  $\mathcal{D}_{\text{xc}}$ , which is particularly important for the gap in Mott insulators [13, 14]. However, no approximate xc functional to date contains finite  $\mathcal{D}_{\text{xc}}$ . Secondly, Mori-Sánchez, Cohen and Yang investigated another dimension, the spin polarization  $n_\alpha - n_\beta$ , and found that the ground state energy should remain constant with respect to fractional  $n_\alpha - n_\beta$  due to static/nondynamic correlation, or competition of (nearly) degenerate quantum states [15, 16].

To visualize the two conditions together, the exact behavior of the Coulomb interactions  $E_{\text{ee}}$  of isolated  $s$ -electrons with different occupancy  $(n_\alpha, n_\beta)$  is shown in Fig. 1b (see also Fig. 1 of Ref. 14), where  $E_{\text{ee}}$  is linear in  $N_e = n_\alpha + n_\beta$  and constant in  $n_\alpha - n_\beta$ . However, neither local/hybrid functionals [16] nor LDA+ $U$  (Fig. 1c) are able to reproduce the exact behavior. The delocalization errors and static correlation errors of DFT are especially pronounced for open-shell or strongly correlated systems. Together with the lack of explicit discontinuity  $\mathcal{D}_{\text{xc}}$ , they lead to serious difficulties in applying DFT to such systems [17].

In this letter, we propose a remedy, LDA plus density matrix minimization (LDA+DMM). Built from the beginning with the above conditions for the exact ground state total energy in mind, our approach offers significant quantitative improvement in total energies over LDA and LDA+ $U$  for strongly correlated systems. Electronic structure predictions of LDA+DMM overcome qualitatively the failures of LDA and LDA+ $U$  in Mott insulators at a modest computational cost. Next, the DMM model is presented, followed by a case study on a prototypical Mott insulator, KCuF<sub>3</sub>.

Our starting point is an isolated atom with open  $l$ -shell, i.e. the number of electrons  $N_e$  is fractional. Such a quantum system is described by a statistical ensemble used, e.g., in Perdew’s original treatise on fractional  $N_e$  in DFT [11]. The quantum state is formally represented by a block-diagonal density matrix

$$\mathbb{D} = \sum_{\alpha} f_{\alpha} |\Psi_{\alpha}\rangle \langle \Psi_{\alpha}| = \text{diag} \left( D^{(0)}, D^{(1)}, \dots, D^{(4l+2)} \right),$$

with  $0 \leq f_{\alpha} \leq 1$  and  $\Psi_{\alpha}$  being normalized Fock space wavefunctions. Alternatively,  $\mathbb{D}$  consists of sub-matrices  $D^{(N)}$  ( $0 \leq N \leq 4l+2$ ), which are  $N$ -body density matrices defined in the  $C_{4l+2}^N$ -dimensional  $l^N$  sub-space. DMM models the ground state energy of the

electron-electron interactions  $E_{ee}$  by minimization via a variational principle, with the trial variable being the  $2^{4l+2}$ -dimensional block diagonal density matrix  $\mathbb{D}$ . The minimization is constrained: (similar to the Gutzwiller constraints [18]): (1)  $\mathbb{D}$  is normalized and positive semidefinite, and (2) the on-site density matrix (ODM)  $\mathbf{n} = [n_{ij}]$  projected from  $\mathbb{D}$  matches that from Kohn-Sham orbitals  $\sum_{nk} f_{nk} \langle \psi_{nk} | i \rangle \langle j | \psi_{nk} \rangle$ . We therefore propose an on-site Coulomb energy functional of the one-reduced density matrix  $\mathbf{n}$  for a sub-system:

$$E_{ee}^{\text{DMM}}[\mathbf{n}] = \min_{\substack{\mathbb{D} \geq 0, \text{tr } \mathbb{D} = 1, \text{tr } \mathbb{D} \mathbf{N} = \mathbf{n}}} \text{tr } \mathbb{D} \mathbb{V}_{ee} = \min_{\mathbb{D} \geq 0} [\text{tr } \mathbb{D} \mathbb{V}_{ee} - V_{ij}(\text{tr } \mathbb{D} \mathbf{N}_{ij} - n_{ij}) - \epsilon(\text{tr } \mathbb{D} - 1)], \quad (2)$$

where  $2^{4l+2}$  dimensional matrices  $\mathbb{V}_{ee}$  and  $\mathbf{N}_{ij}$  are the matrix elements of the on-site Coulomb  $\hat{v}_{ee}$  and occupancy  $\hat{c}_i^\dagger \hat{c}_j$  operators in the Fock space, respectively, and the Lagrange multiplier matrix  $V_{ij} = \partial E_{ee} / \partial n_{ij}$  acts as a non-local potential.

A key advantage of Eq. (2) is that it constitutes a semidefinite programming (SDP) problem [19, 20], a well-known convex optimization problem [21] that can be solved *uniquely* and *efficiently* with numerical algorithms [22–24], which are capable of minimizing Eq. (2) within few seconds for  $d$ -electrons.

Eq. (2) meets the charge-linearity/spin-constancy conditions exactly for  $s$ -electrons, as shown in Fig. 1b. In contrast, the mean-field approximation  $E_{ee} \approx n_\alpha n_\beta U$  (Fig. 1c) of LDA+ $U$  deviates from the exact  $E_{ee}$  except at integer occupancy.

Fig. 1d further elucidates the physical origin of the exact behavior: static correlation due to the presence of alike atoms. If one artificially turns off such correlation by replacing the many-body density matrix  $\mathbb{D}$ , which describes a quantum system in a *mixed* state, with a many-body wavefunction  $\Psi$  in the Fock space, i.e. a *pure* state, and accordingly replacing the mixed-state average  $\langle A \rangle_{\mathbb{D}} = \text{tr } \mathbb{D} \hat{A}$  of operator  $\hat{A}$  in Eq. (2) with the pure state expectation  $\langle A \rangle_{\Psi} = \langle \Psi | \hat{A} | \Psi \rangle$ , one switches to a pure state picture:

$$E_{ee}^{\text{ps}}[n] = \min_{|\Psi|=1, \langle \hat{c}_i^\dagger \hat{c}_j \rangle_{\Psi} = n_{ij}} \langle \mathbb{V}_{ee} \rangle_{\Psi}. \quad (3)$$

This is equivalent to restricting the search space of  $\mathbb{D}$  to idempotent matrices. The pure state formalism is, again, correct only at integer occupancy (Fig. 1d). Otherwise, the difference from Fig. 1b is striking. At a given  $N_e$ , the pure state formalism strongly favors the maximum amount of spin polarization, even more so than LDA+ $U$ , in dramatic violation of the spin-constancy condition. For example,  $\mathbf{n} = \text{diag}(\frac{1}{2}, \frac{1}{2})$  corresponds to the  $N_e = 1$  mixed state

$D^{(1)} = \frac{1}{2} \sum_{\sigma} |\sigma\rangle\langle\sigma|$  with  $E_{ee} = 0$ , or to the pure state  $\Psi = (| \rangle + |\alpha, \beta\rangle)/\sqrt{2}$  with  $E_{ee} = U/2$ . Note that  $D^{(1)}$  may become a pure state in an enlarged space encompassing another atom. This justifies our choice of the many-body density matrix  $\mathbb{D}$  representing an ensemble as the basic variational variable.

DMM is applicable beyond  $s$ -electrons. Fig. 2 shows  $E_{ee}^{\text{DMM}}$  vs.  $(n_{\alpha}, n_{\beta})$  for  $l = 1, 2$  with  $n_{ij} = n_{\sigma} \delta_{ij}$  spherical in each spin channel. Similar to  $l = 0$ , Eq. (2) satisfies the conditions for fractional charge and spin. Fig. 2a-c shows the piecewise straight line  $E_L(N_e) = E_{ee}^{\text{DMM}}$ , as expected of the ground state energy of fractional  $N_e$  [11]. The calculated potential  $V_{ij} = V_L \delta_{ij}$  is spherical, spin-independent, and piecewise constant (dashed lines). An *explicit* derivative discontinuity  $\mathcal{D}_{xc} = V_{\text{ave}}(z_e + \delta) - V_{\text{ave}}(z_e - \delta)$  at integer  $z_e$  is recovered:

$$\lim_{N_e \rightarrow z_e^+} V_{ij} - \lim_{N_e \rightarrow z_e^-} V_{ij} = \mathcal{D}_{xc} \delta_{ij} = [U - x(\mathbf{n})J] \delta_{ij}, \quad (4)$$

where  $V_{\text{ave}} = \text{tr } \mathbf{V} / (4l + 2)$  is the average potential and  $x$  is a coefficient for  $J$ .

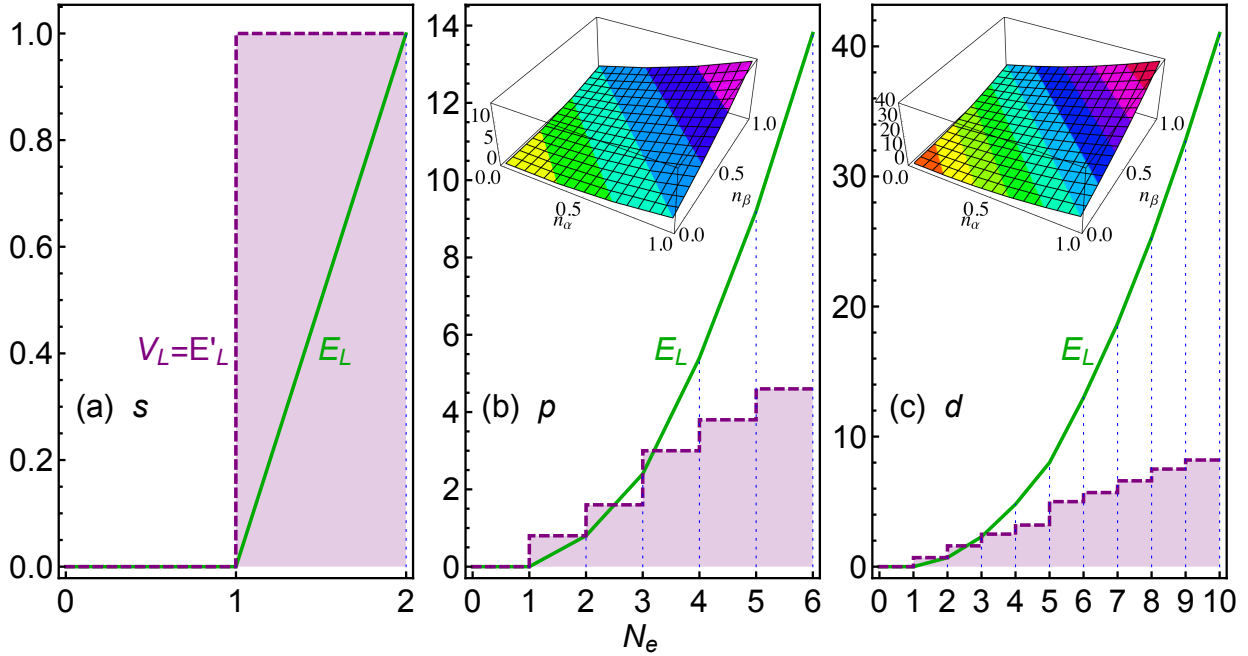


FIG. 2. With  $\mathbf{n} = \text{diag}(n_{\alpha}, \dots, n_{\alpha}, n_{\beta}, \dots, n_{\beta})$ ,  $U=1$ ,  $J=0.2$ , energy  $E_L(N_e) = E_{ee}^{\text{DMM}}(\mathbf{n})$  (solid line) and potential  $V_L = dE_L(N_e)/dN_e$  (purple dashed line) vs.  $N_e$  for  $l = 0-2$ , respectively. Inset:  $E_{ee}^{\text{DMM}}$  vs.  $n_{\alpha}, n_{\beta}$ .

All the above examples fall on the ground state line  $E_L$ , suggesting that the supplied ODMs  $\mathbf{n}$  can be interpolated by those of atomic ground states. We call  $\mathbf{n}$  *linear representable*

if  $E_{ee}^{\text{DMM}}[\mathbf{n}] = E_L(N_e)$ . However, these examples are the exception rather than the norm. For  $l > 0$ , it is generally not possible to interpolate an arbitrary  $\mathbf{n}$  with ground state ODMs alone, i.e.  $E_{ee}^{\text{DMM}}[\mathbf{n}] > E_L(N_e)$ . This can be seen from Fig. 3 showing the energy of random diagonal ODMs. For  $l = 1$  and  $1 < N_e < 5$  (Fig. 3a), the energy of a large number of ODMs is above  $E_L$ , i.e. not linear representable. The same holds for  $l = 2$  and  $1 < N_e < 9$  (Fig. 3b). For a  $p^2$  example of  $\mathbf{n} = \text{diag}(1, 0, 0, 1, 0, 0)$ , which violates Hund's first rule,  $E_{ee}^{\text{DMM}}[\mathbf{n}] = U + 0.8J > E_L(2) = U - J$ . Exceptions include the trivial case of  $N_e \leq 1$  or  $N_e \geq M - 1$  (and hence any  $s$ -system), where the degeneracy of a single electron/hole means no excited states, as well as special  $n$  such as the previous spin-spherical  $n_{ij} = n_\sigma \delta_{ij}$ .

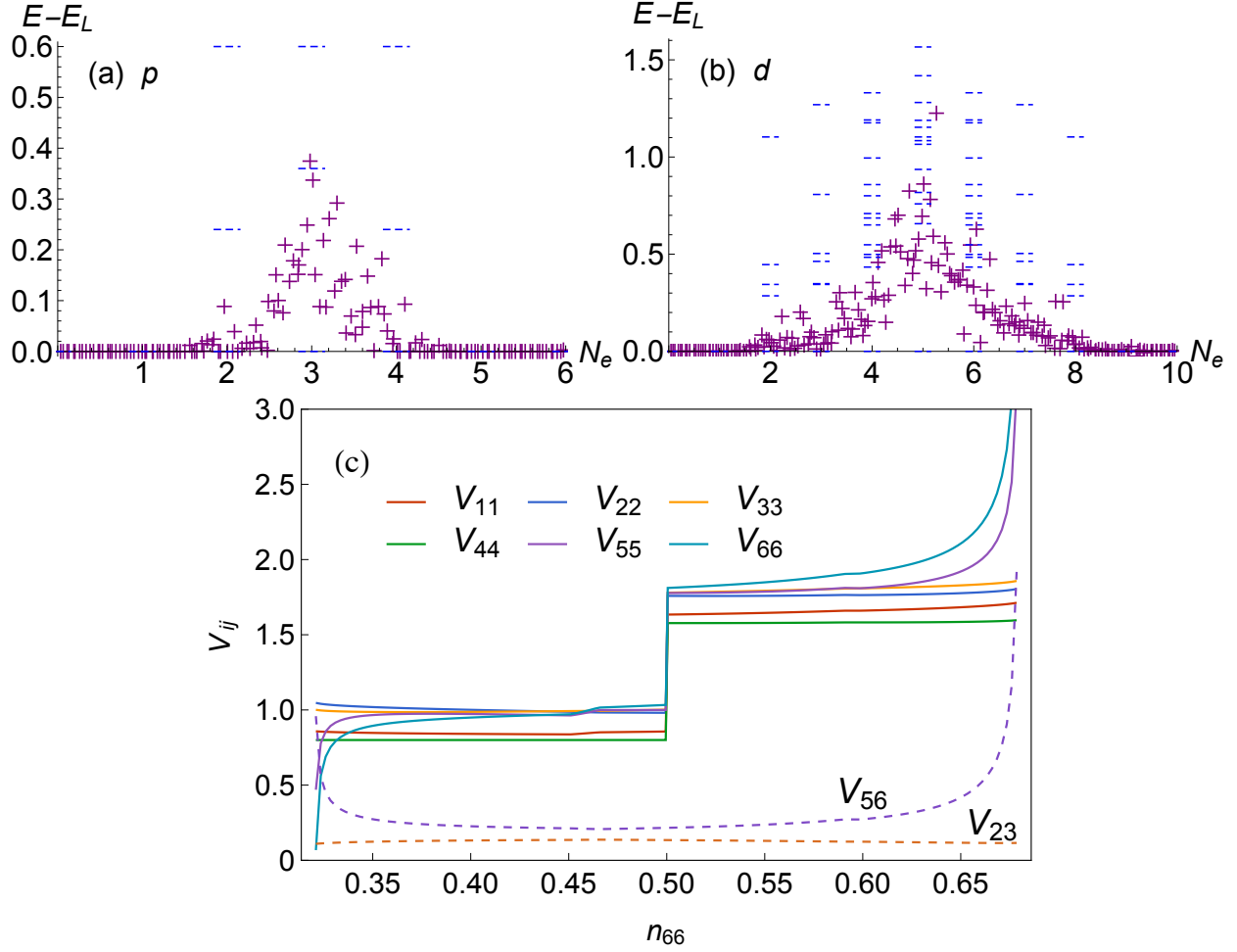


FIG. 3. With  $U=1$ ,  $J=0.2$ ,  $E_{ee}^{\text{DMM}}$  of (a)  $p$  and (b)  $d$ -electrons with random diagonal  $\mathbf{n}$  vs.  $N_e$ , with eigen-energies of  $\mathbb{V}_{ee}^N$  shown as dashed lines; and (c)  $V_{ij}$  for  $l = 1$ ,  $\mathbf{n} = \text{diag}(0.1, 0.2, 0.3, 0.4, \begin{bmatrix} 0.5 & 0.4 \\ 0.4 & n_{66} \end{bmatrix})$  vs.  $n_{66}$ .

Note that in the above linear representable examples in Fig. 2,  $\mathbf{V} = V_L \mathbb{1}$  was found spherical and spin-independent. It can be shown that this is true for any linear representable ODM, not considering discontinuity such as integer  $N_e$ . The physical meaning of  $\mathbf{V} = V_L \mathbb{1}$  is remarkable: essentially, the ground state can be reproduced with a spin-independent potential, as it should be in true DFT. This is not the case for LDA+ $U$ . Now the DMM energy  $E_{ee}$  can be understood as the ground state  $E_L$  plus a penalty for departure from linear representability. Similarly  $\mathbf{V}$  is composed of a scalar part  $V_L$ , plus an aspherical contribution driving the ODM towards linear representability and compatibility with Hund's rules. For example, the dependence of  $\mathbf{V}$  on  $n_{66}$  is shown in Fig. 3c, with a uniform derivative discontinuity  $\mathcal{D}_{xc}$  as in Eq. (4) at  $z_e = 2$ , and singularity in  $V_{55}$ ,  $V_{56}$ ,  $V_{66}$  when an eigenvalue of  $\mathbf{n}$  approaches 0 or 1.

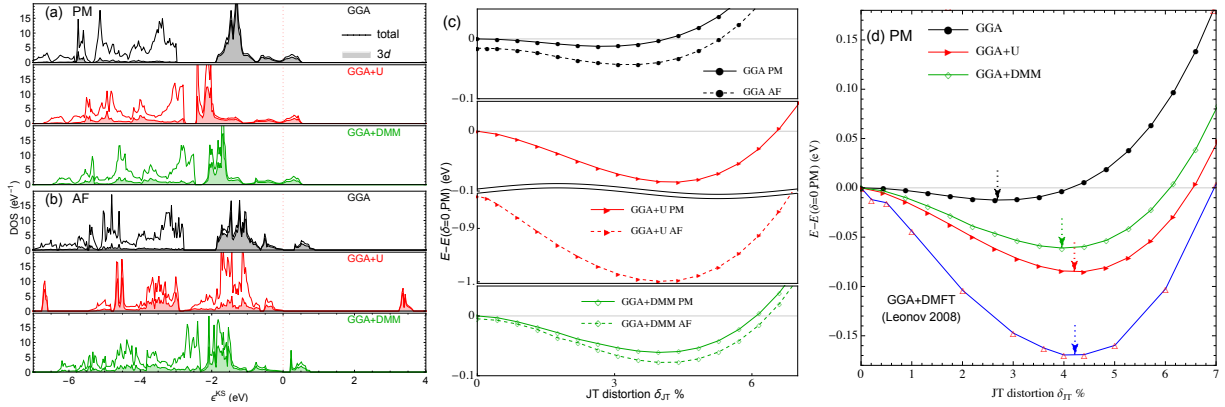


FIG. 4. For  $\text{KCuF}_3$ : density of states in the (a) paramagnetic and (b) antiferromagnetic phase, and energy per formula unit versus Jahn-Teller distortion (c) in the two phases and (d) in PM compared to GGA+DMFT results from Ref. 25. The optimized distortion is pointed out by arrows.

Next, the DMM model will be embedded in DFT calculations for  $\text{KCuF}_3$ , a prototypical Mott insulator. Correct reproduction of Mott-Hubbard gap, orbital ordering and Jahn-Teller distortion in the antiferromagnetic (AF) phase of  $\text{KCuF}_3$  was one of the early achievements of LDA+ $U$  [26]. Leonov and coworkers [25] studied the paramagnetic (PM) phase, which was beyond the capabilities of LDA+ $U$  due to strong static correlation, with DFT+DMFT calculations, and successfully reproduced the experimental Jahn-Teller distortion (4.4% [27]). Note that with  $3d^9$  Cu the AF/PM configurations can be roughly approximated with hole occupancy  $(n_\alpha, n_\beta) = (1, 0) / (\frac{1}{2}, \frac{1}{2})$ , and the discussions following Eq. (3) apply.

The LDA+DMM method for correlated sites  $\{I\}$  is

$$E_{\text{LDA+DMM}} = E_{\text{LDA}} + \sum_I E_{\text{ee}}^{\text{DMM}}[\mathbf{n}^I] - E_{\text{dc}}[\mathbf{n}^I]. \quad (5)$$

We adopt the double counting (dc) scheme of our previous works [28] by separating the dc energy into the Hartree energy and the xc contribution in order to avoid aspherical self-interaction errors:

$$E_{\text{dc}}[\mathbf{n}] = E_{\text{H}}[\mathbf{n}] + E_{\text{dc}}^{\text{xc}}[\mathbf{n}], \quad (6)$$

$$E_{\text{H}} = \frac{1}{2} \sum_{\{m\}} \langle m, m'' | \hat{v}_{\text{ee}} | m', m''' \rangle n_{mm'} n_{m''m'''}, \quad (7)$$

$$E_{\text{dc}}^{\text{xc}} = -\frac{1}{2} [U N_{\text{e}} + J N_{\text{e}} (N_{\text{e}} - 2) / 4]. \quad (8)$$

This allows one to correct the xc energy, not the Hartree term, which is exact by definition in DFT and does not need a dc approximation [28].  $E_{\text{dc}}^{\text{xc}}$  in Eq. (8) is the one used in Ref. 25. Accordingly the correction potential is

$$\Delta V_{ij} = V_{ij} - \partial E_{\text{H}} / \partial n_{ij} - \partial E_{\text{dc}}^{\text{xc}} / \partial n_{ij}. \quad (9)$$

Before delving into numerical details, we point out a salient feature of LDA+DMM. In the so-called spherically averaged or  $J = 0$  limit, Eq. (2) is simply linear interpolation of  $U z_{\text{e}}(z_{\text{e}} - 1)/2$  between integers  $z_{\text{e}}$ , and Eq. (5) becomes

$$E_{\text{LDA+DMM}} = E_{\text{LDA}} + \sum_I U f_{\text{e}}(1 - f_{\text{e}})/2, \quad (10)$$

where  $0 \leq f_{\text{e}} < 1$  and  $N_{\text{e}} = z_{\text{e}} + f_{\text{e}}$ . This is exactly the well-known self-interaction correction for fractional number of electrons (Fig. 1a). In this simplified picture, LDA+DMM corrects the convexity of LDA, in contrast to the mean-field LDA+ $U$ , which corrects for occupancy of each orbital with  $\sum_i U n_i(1 - n_i)/2$ , the root cause of its multiple minima problems. When the  $U$  parameter is large enough,  $N_{\text{e}}$  is pinned to  $z_{\text{e}}$  accompanied by an abrupt derivative discontinuity  $\mathcal{D}_{\text{xc}} = U$  from Eq. (4).

This is indeed observed in our GGA+DMM calculations for  $\text{KCuF}_3$  ( $U_{\text{critical}}=8.06$  eV at  $J=0.9$  eV [29]). Fig. 4ab compares the obtained total and projected density of states (DOS) with GGA and GGA+ $U$ . GGA predicts metallicity in the PM phase. Both GGA+ $U$  and GGA+DMM push occupied  $3d$  states down with no KS gap. The difference is, while the former cannot handle static correlation, GGA+DMM predicts correctly a Mott gap of

$\mathcal{D}_{xc} \approx 7$  eV according to Eqs. (1,4). Note that GGA+DMFT predicts a much smaller band gap  $\sim 1.5 - 3.5$  eV [25]. In the AF phase (Fig. 4b), all methods were able to stabilize antiferromagnetic holes. Both GGA and GGA+DMM predict a tiny KS gap ( $\sim 0.3$  eV). The latter again should be augmented by  $\mathcal{D}_{xc}$ . GGA+ $U$  predicts a larger KS gap of 3.2 eV. Of the three methods, only GGA+DMM was able to predict a Mott insulator for both magnetic configurations.

The total energy properties are more interesting. Fig. 4c compares the energy profile for the PM (solid line) and AF (dashed line) configurations vs. the  $\delta_{JT}$  parameter [25] for the degree of Jahn-Teller distortion. The reference point was chosen as the paramagnetic, undistorted ( $\delta_{JT} = 0$ , space group P4/mmm) structure. All the methods predict correctly the AF ground state. Quantitatively, both GGA and GGA+DMM predict slightly more stable AF state, in qualitative agreement with the low Néel temperature of 38 K. In contrast, GGA+ $U$  penalizes the PM configuration too heavily, in overall agreement with previous LDA+ $U$  studies [30], due to lack of treatment for static correlation.

Finally, the PM energy profiles are compared in Fig. 4d, together with GGA+DMFT results from Ref. 25. Together with Fig. 4c, one observes that GGA stabilization of JT distortion is much too weak, particularly in the PM phase. Both GGA+ $U$  and GGA+DMM predict much larger stabilization energy and amount distortion:  $\delta_{JT} = 4.0\%$  and  $4.2\%$ , respectively, in good agreement with experimental  $4.4\%$ . GGA+DMFT predicts similar distortion with even stronger stabilization energy than the former two. There is yet no clear experimental data to establish quantitatively the JT distortion energy.

In conclusion, built with the exact behavior of the ground state total energy of electrons in mind, LDA+DMM offers unified treatment of derivative discontinuity, delocalization errors and static correlation errors in density functional calculations, with clear advantage over LDA and LDA+ $U$  for strongly correlated systems. As the first generally applicable method to incorporate explicit derivative discontinuity, LDA+DMM correctly reproduced the Mott-Hubbard gap, even in the presence of strong static correlation, as well as more accurate total energies. The fact that DMM is easy to add in any DFT code implementing LDA+ $U$  and that the underlying semidefinite programming problem can be solved uniquely and efficiently, makes it especially attractive. Furthermore, LDA+DMM provides physical insight into the requirements for incorporating the derivative discontinuity and correcting the static correlation and delocalization errors of the current xc functionals. We expect that this

method will be a useful tool for future DFT-based studies of strongly correlated materials.

We acknowledge helpful discussions with L. Vandenberghe, B. O'Donoghue and B. Sadigh. The work of F.Z was supported by the Laboratory Directed Research and Development program at Lawrence Livermore National Laboratory and the Critical Materials Institute, an Energy Innovation Hub funded by the U.S. Department of Energy, Office of Energy Efficiency and Renewable Energy, Advanced Manufacturing Office, and performed under the auspices of the U.S. Department of Energy by LLNL under Contract DE-AC52-07NA27344. V.O. was supported by the U.S. Department of Energy, Office of Science, Basic Energy Sciences, under Grant DE-FG02-07ER46433. We acknowledge use of computational resources from the National Energy Research Scientific Computing Center, which is supported by the Office of Science of the U.S. Department of Energy under Contract No. DE-AC02-05CH11231.

---

\* zhou6@llnl.gov

† vidvuds.ozolins@yale.edu

- [1] V. I. Anisimov, *Strong coulomb correlations in electronic structure calculations : beyond the local density approximation*, Advances in condensed matter science (Gordon and Breach, Amsterdam, Netherlands, 2000).
- [2] V. Anisimov and Y. Izyumov, *Electronic Structure of Strongly Correlated Materials*, Springer Series in Solid-State Sciences (Springer, 2010).
- [3] A. J. Cohen, P. Mori-Sánchez, and W. Yang, *Science* **321**, 792 (2008).
- [4] V. I. Anisimov, J. Zaanen, and O. K. Andersen, *Phys. Rev. B* **44**, 943 (1991).
- [5] A. Georges, G. Kotliar, W. Krauth, and M. Rozenberg, *Rev. Mod. Phys.* **68**, 13 (1996).
- [6] G. Kotliar, S. Y. Savrasov, K. Haule, V. S. Oudovenko, O. Parcollet, and C. A. Marianetti, *Rev. Mod. Phys.* **78**, 865 (2006).
- [7] K. M. Ho, J. Schmalian, and C. Z. Wang, *Phys. Rev. B* **77**, 073101 (2008).
- [8] X. Deng, X. Dai, and Z. Fang, *Epl-Europhys Lett* **83**, 37008 (2008); X. Deng, L. Wang, X. Dai, and Z. Fang, *Phys. Rev. B* **79**, 075114 (2009).
- [9] We use the name LDA for (semi)local xc functionals in general.
- [10] N. Lanata, Y. Yao, C. Z. Wang, K. M. Ho, and G. Kotliar, *Phys. Rev. X* **5**, 011008 (2015).
- [11] J. P. Perdew, R. Parr, M. Levy, and J. Balduz, *Phys. Rev. Lett.* **49**, 1691 (1982).

- [12] L. J. Sham and M. Schlüter, Phys. Rev. Lett. **51**, 1888 (1983).
- [13] J. P. Perdew and M. Levy, Phys. Rev. Lett. **51**, 1884 (1983).
- [14] P. Mori-Sánchez, A. Cohen, and W. Yang, Phys. Rev. Lett. **100**, 146401 (2008).
- [15] A. J. Cohen, P. Mori-Sánchez, and W. Yang, J. Chem. Phys. **129**, 121104 (2008).
- [16] P. Mori-Sánchez, A. J. Cohen, and W. Yang, Phys. Rev. Lett. **102**, 066403 (2009).
- [17] A. J. Cohen, P. Mori-Sánchez, and W. Yang, Chem. Rev. **112**, 289 (2012).
- [18] J. Bünenmann, W. Weber, and F. Gebhard, Phys. Rev. B **57**, 6896 (1998).
- [19] L. Vandenberghe and S. Boyd, SIAM Rev. **38**, 49 (1996).
- [20] M. J. Todd, Acta Numerica **10**, 515 (2001).
- [21] S. Boyd and L. Vandenberghe, *Convex Optimization* (Cambridge University Press, Cambridge, 2004).
- [22] H. Wolkowicz, R. Saigal, and L. Vandenberghe, *Handbook of Semidefinite Programming: Theory, Algorithms, and Applications*, International Series in Operations Research & Management Science (Springer US, 2000).
- [23] R. D. C. Monteiro, Mathematical Programming **97**, 209 (2003).
- [24] B. Borchers, Optim. Methods Softw. **11**, 613 (1999).
- [25] I. Leonov, N. Binggeli, D. Korotin, V. I. Anisimov, N. Stojic, and D. Vollhardt, Phys. Rev. Lett. **101**, 096405 (2008).
- [26] A. I. Liechtenstein, V. I. Anisimov, and J. Zaanen, Phys. Rev. B **52**, R5467 (1995).
- [27] R. H. Buttner, E. N. Maslen, and N. Spadaccini, Acta Cryst. B **46**, 131 (1990).
- [28] F. Zhou and V. Ozolins, Phys. Rev. B **80**, 125127 (2009); **83**, 085106 (2011); **85**, 075124 (2012).
- [29] See Supplemental Material for details.
- [30] N. Binggeli and M. Altarelli, Phys. Rev. B **70**, 085117 (2004).